Biomass Conversion and Biorefinery
https://doi.org/10.1007/s13399-024-05906-6

ORIGINAL ARTICLE

Optimizing selected quality metrics of rice husk briquettes: a response surface methodology approach

S. U. Yunusa[1,2] · E. Mensah[3] · K. Preko[4] · S. Narra[5] · A. Saleh[2] · I. B. Dalha[2] · M. Abdulsalam[2]

Received: 8 April 2024 / Revised: 19 June 2024 / Accepted: 29 June 2024

Abstract

Rice husk is among the most generated biomass residues in developing countries. If this abundant resource is effectively valorized into fuel briquettes, the rate of deforestation and energy deficit in the region would be substantially reduced. In this paper, a process-based modeling was employed to optimize the quality metrics of briquettes made from rice husk as a measure of improving its efficiency and sustainability as an energy source. Two novel bio-binders (locust bean pulp and sweet potato peel) were assessed alongside cassava starch using a low-pressure technique. The experiment was designed using Box Behnken Design (BBD) in Design Expert 13 and Response Surface Methodology (RSM) was employed in optimizing the process metrics and response variables. A confirmatory test was employed to validate the optimal conditions. From the experimental results obtained, the compressed density is between 0.495 and 0.691 g/cm^3, while the impact resistance is between 12.5 and 100%. The optimum process metrics predicted by the model are a 15% binder ratio, 1.1-mm-particle size rice husk, 0.5-min dwell time, and cassava starch binder. The optimal predicted responses are 0.689 g/cm^3 compressed density and 109.6% impact resistance. The differences between the experimented and predicted values were statistically insignificant at a 95% confidence interval. Thus, the study affirms that under the above optimum conditions, rice husk briquettes suitable for domestic application can be sustainably produced. The above findings can serve as a reference in future studies and applications involving briquette production.

Keywords Rice husk · Briquette · Energy · Optimization · RSM

1 Introduction

Over one-third of the global population lives in energy poverty [1]. This is mainly because many people cannot afford or access clean energy. With this, the dependence on solid fuels, especially fuelwood and charcoal, has increased rapidly in recent years resulting in a higher rate of deforestation [2]. About 10 million ha of forest is lost annually between 2015 and 2020, of which, if not halted, about 3.6 gigatons of carbon dioxide equivalent ($GtCO_2$) will be released into the atmosphere between 2020 and 2050 [3]. On this basis, a sustainable solution that would help decrease deforestation and improve energy security is pertinent.

Biomass, being a renewable energy resource abundantly available across the globe [4], has a substantial potential for energy production using various valorization techniques [5]. Rice husk is one major biomass produced globally because rice is a significant dietary staple [6]. Globally, rice husk has an estimated energy potential of about 16 EJ/a [7]. Nigeria is the largest producer of rice in Africa. The country's production capacity increased from 4.0 million tons in 2018 to 8.4 million tons in 2021 [8]. In every kilogram of milled paddy, about 0.28 kg of rice husk is generated [9]. On this basis, about 2.4 million tons of rice husk is produced annually in Nigeria. However, there is still no definite strategy for managing or recycling the generated waste [10]. They are commonly landfilled or burned, contributing to the emission

✉ S. U. Yunusa
suleimanyunusa001@gmail.com; suyunusa@abu.edu.ng

1 WASCAL Graduate Research Programme on Climate Change and Land Use, Department of Civil Engineering, KNUST, Kumasi, Ghana

2 Department of Agricultural and Bio-Resources Engineering, Ahmadu Bello University, Zaria, Nigeria

3 Department of Agricultural and Biosystems Engineering, KNUST, Kumasi, Ghana

4 Department of Physics, KNUST, Kumasi, Ghana

5 Professorship for Material and Energy Valorization, University of Rostock, 18059 Rostock, Germany

Published online: 12 July 2024

of greenhouse gases. Thus, transforming these biomass residues into energy is a means of achieving carbon neutrality and mitigating climate change [11].

One of the common and major techniques employed in harnessing energy from biomass in most developing countries is through briquette production. This involves the compression of raw biomass into a solid, uniformly stable, and more compact form [12]. Through this process, the density and energy content of the biomass is improved [13]. Although the technology was primarily developed to solve the problem of excess waste generation, it is now majorly focused on energy production [14]. Being a solid fuel with good energy content, biomass briquette has the potential to substantially reduce the use of fuelwood and charcoal, especially when used in improved cookstoves [15]. This equally conforms with the principles of waste management in ensuring the reuse, reduction, and recycling of waste materials [16]. The progress in briquette production has been quite slow owing to the high capital cost of setting up a briquetting plant or having a high-pressure machine [16]. On this basis, low-pressure technologies were developed to save cost and promote the use of biomass residues in place of continuous deforestation for fuel. However, another challenging aspect of using the low-pressured press has been the selection of an appropriate and affordable binder. Binding materials are essential in briquetting as they enhance bonding and contribute to both the briquette's physical and combustion performance, especially in low-pressured briquetting. Over the years, starchy binders generated from edible products such as cassava, flour, corn, wheat, and potato, have been the most used binders in briquetting [17]. They are, however, expensive and have low water resistance [17]. Another form of binders is the inorganic binders which are grossly used for their hydrophobic and strength properties [18]. They are, however, producing high ash content [19]. Hence, studies have now focused on developing novel, affordable, and more sustainable binders [20]. In this paper, two novel binders (sweet potato peel gelatinized with locust bean husk solution, and locust bean pulp) were evaluated alongside cassava starch.

Several studies have examined the properties of briquettes under varying process parameters. This includes Brunerová et al. [16] where a low-pressured (< 5 MPa) technology was employed in densifying four biomass residues using wastepaper pulp as a binder. The developed briquettes have densities between 179.69 and 227.53 kg/m^3 at varying mixing ratios. Magnago et al. [21] produced briquettes from the blends of citrus peels and rice husks using grounded Irish potato peel as a binder. The briquettes have densities between 0.35 and 0.46 g/cm^3, ash content between 3.9% and 4.9%, and gross calorific value between 14.6 and 17.2 MJ/kg. Yank et al. [22] developed briquettes from rice husk and bran using three types of binders (cassava wastewater, rice dust, and okra stem gum). The results show that the briquettes produced with cassava starch wastewater had the highest density of 471.3 kg m^{-3}, while briquettes produced from rice dust had the highest durability of 91.9% and compressive strength of 2.54 kN. Similarly, Sunnu et al. [23] produced and characterized charred briquettes made from rice husk, maize cobs, palm kernel shells, and sawdust at variable process parameters. The briquette made with palm kernel shell with 0.60 mm particle sizes, densified at 30 MPa had the best performance with an ash content of 2.7% and relaxed density of 753 kg/m^3.

Similarly, some recent studies that explored optimization include Oladosu et al. [24] where the optimum thermal parameters of briquettes produced from the flamboyant pod and corn cob bonded with cassava starch were determined. An optimum ignition time, boiling time, and burning rate of 185 s, 930 s, and 0.032 g/s, respectively, were recorded. In a different approach, Nganko et al. [25] observed that a binder ratio, pressure and dwell time of 10%, 75 kPa, and 7.49 min are optimum for producing carbonized sawdust briquettes. For lignite powder, Guo et al. [26] reported an optimum compression pressure, binder ratio, water, and drying time of 19.70 MPa, 0.52%, 21.61%, and 5.65 h, respectively. For briquettes made from urban wood waste and poultry litter, a 1:1 mixing ratio and 194-s dwell time were found to be optimum, yielding HHV of 22.75 MJ/kg and a density of 1180.4 kg/m^3 [27]. Overall, previous studies reported an optimum binder and compression pressure of < 5–15% and 6.86 – 122.7 MPa for different biomass materials [28].

While studies have explored the production and analysis of briquettes from several biomass [28], there is no study on briquette production using uncarbonized rice husk at low pressure (≤ 5 MPa). This stems from some perceptions that rice husk is unsuitable for briquette production due to its high ash and silica content. This belief has over the years reduced the potential of this abundant resource, especially in developing countries. With this, only a few studies utilized rice husk in briquette production. These were largely employed as co-feedstock with other biomass as in the studies of Yank et al. [22] and Magnago et al. [21], or in carbonized form [29, 30], or using a higher compression pressure which is generally expensive. Thus, this paper aims to develop briquettes from uncarbonized rice husk at low pressure and optimize the process and quality variables to improve its efficiency. In addition to providing the optimum conditions, another novelty of the paper is that it assessed the potential of some biomass materials as novel binders in briquette production. This will serve as a way of saving costs, thereby making it affordable and accessible to low-income households. Overall, the data obtained from this paper will provide a guide for the sustainable and efficient utilization of rice husk as an energy source.

2 Materials and methods

2.1 Materials

The materials used are as follows:

a. ***Rice husk***: this is the major outturn after milling paddy rice. Depending on the type of milling employed (i.e., one-stage or two-stage), rice husk comes in two forms, i.e., one-stage and two-stage rice husk. The rice husk used in this study is a two-stage rice husk. This type of rice husk is obtained from two-stage milling. Two-stage milling involves the removal of the rice husk and bran separately [31].
b. ***Sweet potato peel:*** sweet potato (*Ipomoea batatas* L.) peel is the bark obtained after peeling off the potato. Although it has some nutritional value, it is largely considered a waste material. Sweet potato is largely available in Nigeria as it is among the major crops cultivated [32].
c. ***locust bean pulp and husk:*** Locust bean pulp and husks are obtained from the fruit of the African locust bean (*Parkia biglobosa)* tree. This is a perennial tree of leguminous origin that belongs to the sub-family *mimosoideae,* and family *leguminosae* (now family *fabaceae*) [11]. It is a native African tree predominant in nineteen African countries including Nigeria [33]. This resource is largely available in Nigeria, especially in the Northern part of the country. A matured African locust bean tree yields more than a tone of fruits [34]. In Nigeria, the seeds of the fruit are commonly processed into a local seasoning referred to as *Dawa Dawa*, while the pulp and husk have very limited applications [12], therefore they end up as waste or as animal fodder.

A pictorial view of these materials is presented in Fig. 3. Rice husks weighing 40 kg were obtained from a rice mill in Kaduna State, Nigeria (latitude 11°12′1.8″ N and longitude 7°33′23.2″ E). The binding feedstocks viz: sweet potato peel (PPL), locust bean husk (LBH), and locust bean pulp (LBP) were sourced from Samaru (latitude 11°10′5.65824″ N and longitude 7°39′25.88832″ E), and Sabon Gari, Zaria, Kaduna State, Nigeria (latitude 11°6′37.1826″ N and longitude 7°43′40.48392″ E, and latitude 11°6′28.54044″ N and longitude 7°43′47.84988″ E), respectively. The control binder (cassava starch) was purchased from the market.

2.1.1 Material preparation

All samples were screened for foreign materials and kept in a medium-density polyethylene (MDPE) plastic to avoid moisture absorption. The rice husk was not dried further as it was well dried (MC = 4.8%). However, due to its recalcitrant nature resulting from its high silica and ash content, it was milled to smaller particle sizes of ≤ 2000 microns (2 mm) using a hammer mill (Model HR600, Henan, China) fitted with a 2-mm screen mesh and powered by a 5.22-kW diesel engine output. Milling the sample will give it better mixing and binding uniformity [35]. Because PPL was obtained in fresh form, it was washed and sun-dried at an average temperature and relative humidity of 29 ℃ and 65% for 5 days. The temperature and relative humidity were measured using a smart sensor (Model AR837, Dongguan Wanchuang Electronic Products, China) with an accuracy of ± 1℃ for temperature measurements and ± 1% for relative humidity measurements. The dried sample was then grounded using an electric milling machine (Model 9z-23, Zhengzhou Shuliy Machinery Company, Ltd., China). LBH was also sun-dried at an average temperature and relative humidity of 29 ℃ and 65% for 2 days and milled using a hammer mill (Model HR600, Henan, China) fitted with a 2-mm screen and powered by a 5.22-kW diesel engine output. Subsequently, the milled sample was sieved through a 1-mm standard sieve (Shaoxing Hengyu Instrument Company, China) to obtain particles ≤ 1 mm. LBP was manually mixed to homogenize the lumps and eventually sieved through a 1 mm sieve size to obtain particles ≤ 1 mm.

2.1.2 Material characterization

The feedstocks were characterized to determine the gross calorific values, volatile matter, ash content, fixed carbon, and elemental constituents like carbon, nitrogen, sulfur, hydrogen, and oxygen. The gross calorific value was determined using a Bomb Calorimeter (Model: 6100, Parr Instrument Company, USA) with a class precision of 0.1 – 0.2%, following the method described in ASTM D5865-10a [36]. The moisture content was estimated using Eq. 1 following the method described in ASTM D3173-87 [37]. Samples were heated in an oven (Model: DHG – 7090A, England) with a temperature control precision of ± 1℃.

$$MC(\%)wb = \frac{W_i - W_f}{W_i} \times 100 \quad (1)$$

where MC (%) wb is moisture content (web basis), W_i is the initial weight of the sample (g), and W_f is the final weight of the sample (g)

The volatile component was determined by heating the samples in a furnace (Model SX-5–12 Box-Resistance, Huanghua Faithful Instrument Co., LTD, China) with a maximum allowable temperature of 1200 ℃, based on the modified procedure described in ASTM D3175-07 [38] for

all sparking fuels. The percentage of volatile matter in each sample was estimated using Eqs. 2 and 3 [38].

$$weight\ loss(\%) = \frac{A-B}{A} \times 100 \tag{2}$$

$$Volatile\ matter(\%) = C - D \tag{3}$$

where C is the weight loss (%), and D is the moisture content (%).

where A is the weight of the oven-dried sample (g) and B is the weight of the sample (g) after heating in the furnace.

The ash content was determined as per ASTM D3174-02 [39] by heating in a furnace (Model SX-5–12 Box-Resistance, Huanghua Faithful Instrument Co., LTD, China) with a maximum allowable temperature of 1200 ℃, and the percentage ash content was estimated using Eq. 4 [40].

$$Ash\ content(\%) = {}^{M_{ash}}/_{M_{oven-dry}} \times 100 \tag{4}$$

where M_{ash} is the mass of the ash (g) and $M_{oven-dry}$ is the mass of the oven-dried sample (g).

The fixed carbon (FC) was estimated by subtracting the percentage of moisture content (MC), volatile matter (VM) and ash content from 100 as given in Eq. 5 [25]

$$\%\ FC = [100 - (\%MC + \%Ash + \%VM)] \tag{5}$$

The nitrogen content was determined using the Micro-Kjeldahl method with a Micro-Kjeldahl digestion distillation apparatus and sulfur content was determined using the aluminum block method in a Tecator digestor (Model 40, Tecator AB, Sweden). The carbon, hydrogen, and oxygen contents were however determined from the result of proximate analysis with an accuracy of ± 2% using Eqs. 6-8 [41].

$$Carbon(\%) = 0.635\text{FC} + 0.460\text{VM} - 0.095\ \text{AC} \tag{6}$$

$$Hydrogen(\%) = 0.059\text{FC} + 0.060\text{VM} + 0.010\text{AC} \tag{7}$$

$$Oxygen(\%) = 0.340\text{FC} + 0.469\text{VM} - 0.023\text{AC} \tag{8}$$

where FC is fixed carbon, AC is ash matter, and VM is volatile matter.

2.2 Experimental design

The experiment was designed using Box Behnken Design (BBD) with three numerical factors (each set at three levels), one categorical factor, and three replicated central points. Box-Behnken Design (BBD) was selected because it is among the two most popular RSM designs (i.e., Central Composite Design CCD and BBD). In addition, it is flexible and easy to obtain as it does not require a test for axial points. Thus, the issue of extreme experimental boundaries is addressed. As depicted in Table 1, the numerical factors considered are binder content (5%, 10%, and 15%), particle size (1 mm, 1.5 mm, and 2 mm), and dwell time (0.5, 1, and 1.5 min), while the categorical factor considered is binder type {Cassava starch (CSS), potato peel gelatinized with locust bean extract (PPL), and locust bean pulp (LBP)}. Fifteen randomized order runs were generated (Table 3) using the Design Expert Software (version 13, Stat-Ease Inc., MN, USA). However, in BBD, the design is duplicated for each combination of the categoric factor levels. Based on this, 45 experimental runs were generated for the three categoric levels (binder types). Two responses (compressed density and impact resistance) were considered, and Response Surface Methodology (RSM) modeling was employed in optimizing the production. The experimental process flowchart is presented in Fig. 1.

Table 1 Actual and coded factors for experimental design

Factors	Code	Variation Levels		
		Low (− 1)	Medium (0)	High (+ 1)
Binder ratio (%)	A	5	10	15
Particle size (mm)	B	1	1.5	2
Dwell time (min)	C	0.5	1	1.5
Binder type	D	PPL	CSS	LBP

The number of experiments in three-level factorial BBD was calculated using Eq. 9 [42].

$$N = 2k(k-1) + cp \tag{9}$$

where cp is the number of central points, k is the number of factors, and N is the number of experiments.

2.3 Binder preparation

a. Binder PPL

Binder PPL is a combination of potato peel and LBH solution. In preparing the binder, 300 g of raw LBH was mixed with 8 L of water at room temperature. The mixture was then boiled continuously with an electric stove until the reddish surface was observed to have turned pale yielding a reddish-brown solution. The pre-processed potato peel was then mixed with 100 ml of water at room temperature until it dissolved into a paste without clogs. The paste was then added to 500 ml of boiled LBH solution and stirred continuously for about 5 min to gelatinize.

b. Binder LBP and CSS

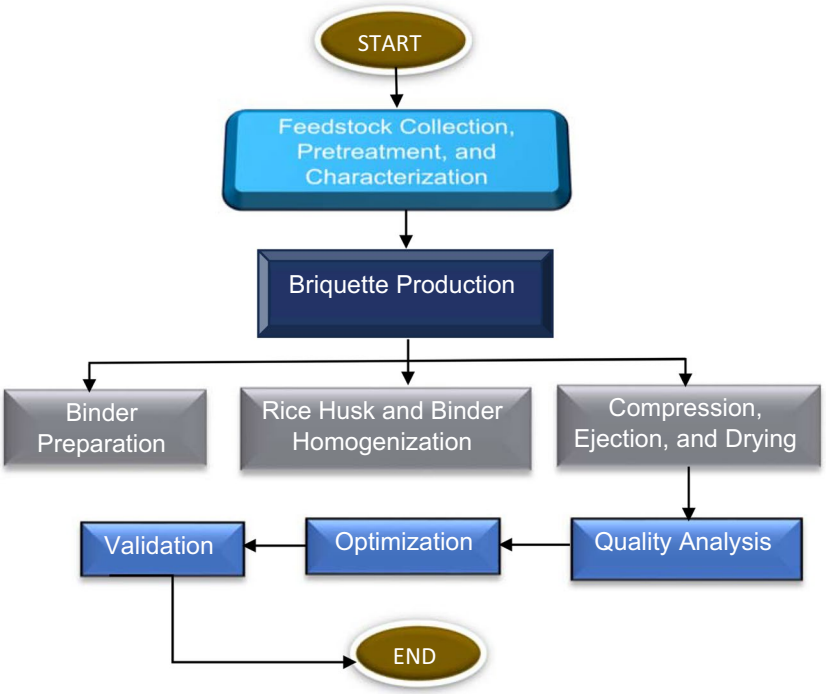

Fig. 1 Experimental process flowchart

In preparing binder LBP and CSS, the raw samples were dissolved into a paste using 100 ml of water at room temperature. 500 ml boiled water was added to the paste and mixed continuously for 5 min to gelatinize appropriately.

2.4 Briquette production

The briquettes were produced with a low-pressure hydraulic piston press with four cylindrical molds of 8-cm diameter and height of 16 cm. The press has a total weight of 100 kg and is made of a combination of galvanized and stainless steel metal. In producing the briquettes, the rice husk was manually mixed with the hot binder for about 10 min to homogenize appropriately. Because the water ratio was not considered a variable, a predetermined constant volume of 140 ml befitting to all the mixing ratios was added and mixed to further improve homogenization and ease compression. A total of 200 g of the sample mixture were fed per mold and compressed at an average room temperature of 28 ℃ and pressure of 4.5 MPa using a 5-ton hydraulic jack. Being a four-cylinder machine, 4 briquette samples were produced per run in triplicate and were sun-dried for a week. The dried samples were kept at room temperature for 23 days to obtain a total relaxation period of 30 days before evaluation. Figure 2 shows the pictorial view of the briquetting press.

Figure 3 shows the pictorial view of the raw and preprocessed feedstocks, and the briquettes produced from each combination. As depicted, the primary feedstock is a

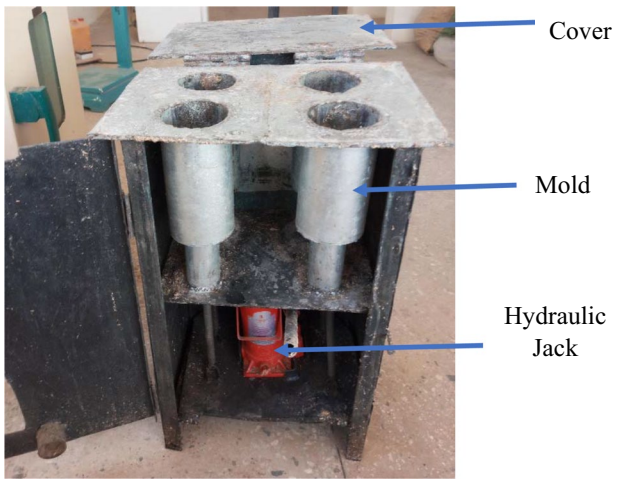

Fig. 2 Briquette production press

stage two rice husk (Fig. 3a), which was milled to ≤ 2 mm (Fig. 3b) to improve interparticle bonding. Other feedstocks are the binding feedstocks, which include the cassava starch as received (Fig. 3c), LBH as received (Fig. 3d.), preprocessed LBH (Fig. 3e), PPL as received (Fig. 3f), preprocessed PPL (Fig. 3g), and LBP as received (Fig. 3h). While briquettes were produced from rice husks and CSS (Fig. 3i), PPL was combined with LBH extract to form a single binder used for producing PPL briquettes (Fig. 3j), and the third binder is LBP which yielded the LBP briquettes (Fig. 3k).

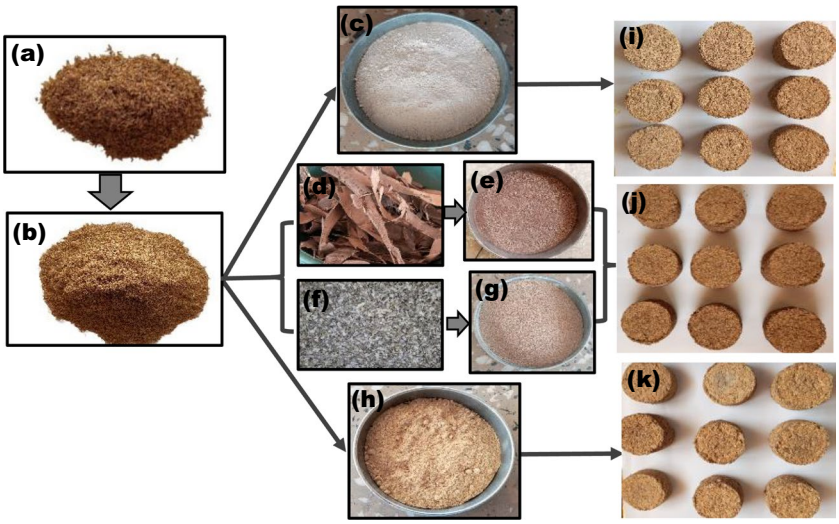

Fig. 3 Feedstocks and developed briquettes. **a** rice husk, **b** milled rice husk, **c** CSS, **d** LBH, **e** milled LBH, **f** PPL, **g** milled PPL, **h**, LBP, **i** CSS briquettes, **j** PPL briquettes, **k** LBP briquettes

2.5 Quality evaluation

The briquettes were tested for compressed density and impact resistance.

2.5.1 Compressed density

The compressed density was determined following ASTM D2395-17 [43]. Compressed density is the ratio of the mass of the briquettes to the corresponding volume after ejection from the mold as given in Eq. 10 [44]. The volume was determined by directly measuring the diameter and length in two perpendicular directions (± 0.01 mm) using a digital vernier caliper and the mass (± 0.1 g) was determined by weighing the samples on a digital scale balance (Model: OPH-T3001, Optima Scale, USA).

$$\rho = \frac{m}{\pi/4 \bullet d^2 l} \tag{10}$$

where ρ is the density (g/cm^3), m is the mass of the briquette (g), d is the averaged diameter (cm), and l is the averaged length (cm).

2.5.2 Impact resistance

The briquette impact resistance test is regarded as the overall best diagnostic of briquette quality [45]. The impact resistance test was carried out as per ASTM D440 – 86 [46]. The samples were dropped from a height of 2 m onto a steel plate. After shattering, the samples were separated based on sized proportions, and only pieces that weighed 5% or more of the initial weight of the briquette were considered in the IRI estimation [47]. The impact resistance index (IRI) was estimated using Eq. 11 [45].

$$IRI = \frac{N}{n} \times 100 \tag{11}$$

where N is the number of drops and n is the number of pieces that weighed 5% or more of the initial weight of the briquette after N drops.

2.6 Uncertainty analysis

Uncertainty analysis measures an instrument's error or result, assesses the fitness of the values obtained and estimates the parameters' accuracy. The uncertainties from this work's known physical values were calculated using Eq. 12 [48].

$$U_r = \left(B_r^2 + P_r^2\right)^{1/2} \tag{12}$$

where U_r is the uncertainty of the parameter at a 5% level of significance, B_r is the systematic uncertainty, and P_r is the random uncertainty. B_r and P_r were determined from Eqs. 13 and 14, respectively.

$$B_r = \left[\sum_{i=1}^{n_5} \left(\frac{1}{r}\frac{\partial r}{\partial X_i} B_i\right)^2\right]^{1/2} r \tag{13}$$

$$P_r = \left[\sum_{i=1}^{n_5} \left(\frac{1}{r}\frac{\partial r}{\partial X_i} p_i\right)^2\right]^{1/2} r \tag{14}$$

where r is the parameter that depends on the variable X_i, Bi is the systematically measured error in r, and pi is the

Table 2 Accuracy and uncertainty of instruments and parameters

Instrument	Parameter	Accuracy	Uncertainty (%)
Smart sensor	Ambient temperature	±1℃	±1.73
Smart sensor	Relative humidity	±1%	±2.26
Digital scale balance	Weight	±0.1 g	±2.13
Vernier caliper	Length	±0.01 mm	±0.09
Vernier caliper	Diameter	±0.01 mm	±0.03
Overall experimental uncertainty			±3.56

measurement level uncertainty in r. For the repeatability of the experiments, the overall experimental uncertainty (σ_k) percentage was calculated using Eq. 15. Hence, the accuracies and uncertainties of the parameters are presented in Table 2. With an overall uncertainty percentage of ± 3.56%, it shows that the findings from the experiment are reliable.

$$\sigma_k = \left[\left(U_{r1}\right)^2 + \left(U_{r2}\right)^2 + \cdots + \left(U_{rn}\right)^2 \right]^{1/2} \quad (15)$$

2.7 Statistical analysis and performance optimization

The experimental data were analyzed using analysis of variance (ANOVA) in Design Expert Software (version 13, Stat-Ease Inc., MN, USA). A second-order polynomial equation (Eq. 16) was employed in predicting the response variables as a function of the independent variables and the various interactions. Response surface methodology (RSM) was employed in optimizing the process parameters and response variables [49].

$$y = \beta_o + \sum_{i=1}^{k} \beta_i x_i + \sum_{i=1}^{k} \beta_{ii} x_i^2 + \sum_{i=1}^{k} \sum_{j=1}^{k} \beta_{ij} x_i x_j \quad (16)$$

where y denotes the response variable, x_i and x_j are the input variables, k the number of factors, β_o is the intercept, β_i is the first-order model coefficient, β_{ii} is the quadratic coefficient, and β_{ij} is the linear model coefficient for the interaction between variables i and j.

3 Results and discussion

3.1 Feedstocks characterization

The results of the feedstock analysis are presented in Table 3. The calorific value of rice husk is 21.78 MJ/kg, consistent with the values (14.2–20.5 MJ/kg) reported by Asamoah et al. [50] for rice husks/straws. The obtained value also meets the European Norm (ENplus) limit of 16.56 MJ/kg and exceeds the typical range (14.7–16.6 MJ/kg) reported in ISO 17225–1 [51], showing that the rice husks have adequate energy content for use as fuel. Because the calorific value is an estimate of the energy content present per unit mass of the sample, it is one of the most important properties in assessing the suitability of biomass as fuel [52]. The binding feedstocks also have good calorific values between 21.26 MJ/kg for PPL and 34.48 MJ/kg for LBP. With all the feedstocks having good calorific value, it indicates that the resultant briquettes would have good energy densities [20]. Similarly, high values of volatile matter were recorded (62.56 –90.9%) indicating the potential of having good ignitability and combustion efficiency [53]. The content of volatile matter obtained agrees with the range (71.4–88.3%) reported for food waste, saw dust, coconut shell, husk, and fiber intended for briquette production[54]. Although the level of ash in the primary feedstock (rice husk) is above the required limit (< 4%) for briquette production [55], the value obtained (12.9%) conforms with the typical range of ash content in rice husks (13–23%) reported in ISO 17225–1 [51]. This is one major limitation in briquetting rice husk [29]. The content of ash in a fuel shows its slagging potential during combustion, therefore, the lower the ash content, the lower the slagging and fouling behavior and the better the heating value [55]. On this basis, applying thermal pretreatment techniques such as hydrothermal carbonization [56], or the use of chemical additives such as $Ca(H_2PO_4)_2$ [57], or organic additives such as guar gums [58], and lignin [59] may reduce the ash level.

With carbon content between 39.59 and 47.37%, oxygen between 36.97 and 43.74%, and hydrogen between 5.18 and 5.72% it shows that the major elemental constituents needed for combustion are adequately present in the feedstocks. The contents of carbon, oxygen, hydrogen, and sulfur obtained in rice husk agrees with the reported range in ISO 17225–1 [51] (Table 2). Apart from the sulfur content of LBP and LBH, other minor elemental constituents (nitrogen and sulfur) are low in the feedstocks, showing lesser potential to emit nitrogen and sulfur when combusted. It is important to note that the lower the nitrogen and sulfur content, the cleaner the fuel during combustion [40].

Table 3 Result of proximate and ultimate analysis

Sample	Moisture content (%)	Volatile matter (%)	Ash content (%)	Fixed carbon (%)	HHV (MJ/kg)	C (%)	N (%)	O (%)	H (%)	S (%)
RH	4.8	78	12.9	4.3	21.78	39.59	1.330	39.999	5.351	0.3232
LBP	6.7	63.18	5.35	24.77	34.48	47.37	0.560	43.10	5.66	7.17
LBH	10	55.56	13.25	24.19	32.45	42.88	1.330	36.97	5.18	7.699
PPL	6.7	84.2	5.5	3.7	21.26	43.64	1.120	43.740	5.724	0.4702
ISO 17225–1 [51]	–	–	13–23	–	14.7 – 16.6	38 – 43	0.1 – 0.8	35 – 47	4.3 – 5.1	0.02 – 0.10

RH rice husk, *LBP* locust bean pulp, *LBH* locust bean husk, *PPL* sweet potato peel. The quoted values of ISO 17225–1 are specifically for the primary biomass (rice husk).

3.2 Experimental design inputs and responses

The experimental design input variables and responses are presented in Table 4. The values of compressed density (CD) range between 0.495 g/cm^3 for LBP and 0.691 g/cm^3 for PPL with close outputs for the three binder types. While impact resistance range between 12.5 and 100% with CSS binder having the highest. The obtained quality values are relatively low because rice husk is a low-density (96–160 kg/m^3) biomass [60], with low lignin reactivity. Therefore, it must be subjected to longer dwell time and higher pressure to consolidate appropriately into higher-quality composites [61, 62]. Moreover, the density of briquette made from a low-pressured hydraulic piston press is usually < 1000 kg/m^3 [63].

While there was no significant difference among the compressed densities of all the briquette types, the change in interaction and binder type reacted differently in some instances. For example, in Fig. 4, the effect of binder ratio on compressed density at constant particle size (2 mm) depicted a different pattern for LBP briquettes. This shows that, as the content of the binder increases, the compressed density increases. This was only observed between the binder ratio of 10% and 15% in CSS and PPL briquettes, which could be because densifying rice husk at room temperature and low pressure requires large amount of binder to attain a quality and durable briquette [22]. However, in the case of CSS and PPL, a slight decrease in compressed density was observed between the binder content of 5% and 10%.. While this may be influenced by the variation in dwell time at the central design point (10% binder), it indicates that an increment in the binder content does not always imply an improvement in briquette quality. Thus, it depends on other interacting factors such as the type of biomass and binder, particle size, and compression pressure, among others. The above assertion is consistent with the findings of Falemara et al. [64] which observed biomass type to influence the density of briquettes even with higher binder ratio (20% and 25%), and Fadele et al. [65] where some samples combination with lower binder content showed better quality. In Fig. 5, the effect of particle size on compressed density is presented. As depicted, the density is higher at the lowest particle size (1 mm) except for briquettes bonded with LBP binder which may be attributed to the binder's coarse texture even when gelatinized. Miao et al. [35] also observed that smaller particle sizes yields briquettes with better quality and thermal performance. Also, because CSS is purely starch and PPL contains a significant amount of starch, they have better gel stability and viscosity following the high content of amylose and amylopectin [20]. Thus, both surface and core layer particles are adequately bonded resulting in better density.

Table 4 Experimental design inputs and responses

Std run	A: BR (%)	B: PS (mm)	C: DT (min)	Responses					
				CD (g/cm^3)			IRI (%)		
				CCS	LBP	PPL	CCS	LBP	PPL
1	5	1	1	0.671	0.637	0.514	12.5	14.3	16.7
2	15	1	1	0.676	0.558	0.691	100.0	50.0	50.0
3	5	2	1	0.592	0.495	0.561	12.5	12.5	33.3
4	15	2	1	0.650	0.571	0.610	100.0	50.0	50.0
5	5	1.5	0.5	0.564	0.570	0.688	33.3	50.0	33.3
6	15	1.5	0.5	0.618	0.655	0.663	33.3	25.0	50.0
7	5	1.5	1.5	0.614	0.668	0.650	12.5	33.3	50.0
8	15	1.5	1.5	0.630	0.596	0.669	50.0	66.7	14.3
9	10	1	0.5	0.551	0.623	0.630	33.3	20.0	50.0
10	10	2	0.5	0.584	0.557	0.529	50.0	50.0	14.3
11	10	1	1.5	0.608	0.665	0.644	33.3	25.0	16.7
12	10	2	1.5	0.591	0.585	0.541	14.3	14.3	16.7
13	10	1.5	1	0.666	0.592	0.636	20.0	25.0	16.7
14	10	1.5	1	0.681	0.580	0.608	50.0	25.0	20.0
15	10	1.5	1	0.657	0.592	0.601	14.3	25.0	25.0

BR binder ratio, *PS* particle size, *DT* dwell time, *CSS* cassava starch, *PPL* sweet potato peel, *LBP* locust bean pulp

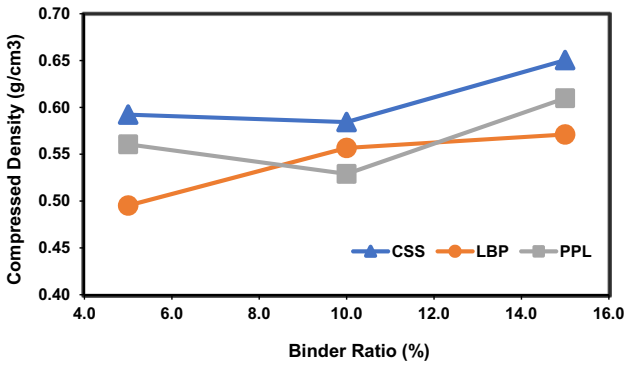

Fig. 4 The effect of binder ratio on compressed density

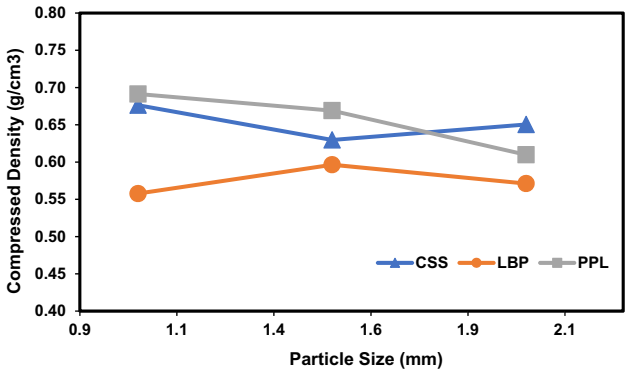

Fig. 5 The effect of particle size on compressed density

This equally applies to impact resistance but is more evident with CSS briquettes, because contrary to the properties recorded immediately after ejection from the mold as in compressed density, sometimes the briquettes' morphology changes drastically after attaining the relaxed (dried) period. Although LBP presented a good compressed density, the strength (impact resistance) of CSS briquettes is significantly better after drying (Fig. 6). This shows that, although density is an essential briquette quality parameter, it does not necessarily imply better durability or strength of the briquette [66]. Thus, as shown in Fig. 7, there is a weak positive correlation between the compressed density and the impact resistance index. The effect of the residence or dwell time is also not consistent as the briquette types

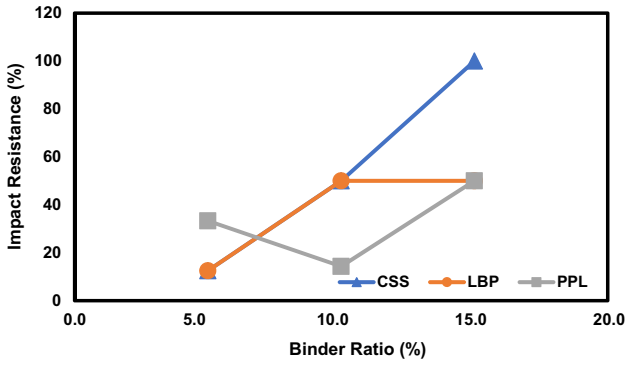

Fig. 6 The effect of binder ratio on impact resistance

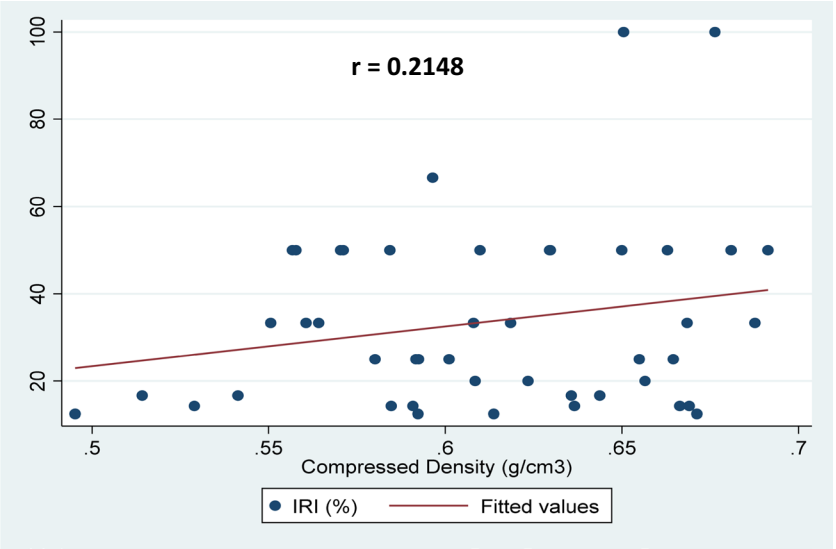

Fig. 7 The correlation plot of impact resistance index and compressed density

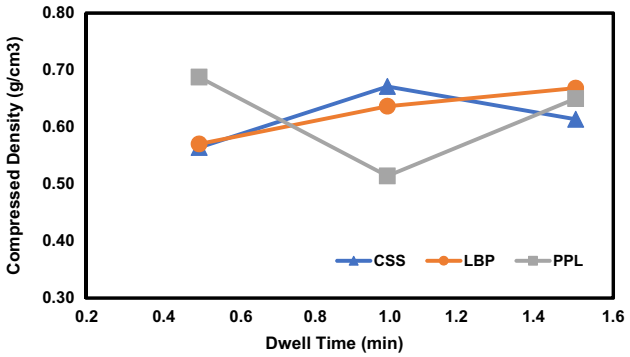

Fig. 8 The effect of dwell time on compressed density

Table 5 Response model fit summary output for compressed density and impact resistance

Indicators	R^2	Adjusted R^2	Predicted R^2	Predicted Precision
Compressed density	0.9572	0.9078	0.8099	15.97
Impact resistance	0.9646	0.9312	0.8453	23.30

react differently (Fig. 8). While this may not accurately describe the impact, it is pertinent to note that due to the less precision in low-pressured or manual briquette production, it is sometimes difficult to establish or examine the change being influenced by the production process factors.

3.3 Analysis of variance and regression model equations

Table 5 presents the fit statistics parameters of the response variables. The r-squared values (0.9578 and 0.9646) are in reasonable agreement with the adjusted r^2 values (0.9078 and 0.93) as the differences between both are less than 0.2. Furthermore, the adequate precision in both responses is desirable as they are greater than 4. This further depicts the adequacy of the model in navigating the design space.

The predicted vs actual plots of compressed density and impact resistance are shown in Fig. 9. As indicated, the data points are closely aligned to the line depicting a strong correlation between the predicted and actual values. These further prove the fitness of the model in navigating subsequent design space.

Tables 6 and 7 show the results of the analysis of variance. The results depict the model's significance level and the lack of fit relative to pure error. In both results, the models have very low p-values (<0.0001), showing that there is only a 0.01% chance that large F-values (19.37 and 28.88) could occur due to noise. This yielded a significant model and insignificant lack of fit, proving minimal variation between the design points and the predicted values.

The regression equations of compressed density (ρ_c) and impact resistance (I) for the independent variables [binder ratio (A), particle size (B), dwell time (C), and binder type] are presented in Eqs. 17-19 with p, c, and l representing PPL, CSS, and LBP binders, respectively. Because the design in BBD is duplicated for each categoric factor level, three equations were generated for each response, with each representing the regression equation of a specific binder type (D).

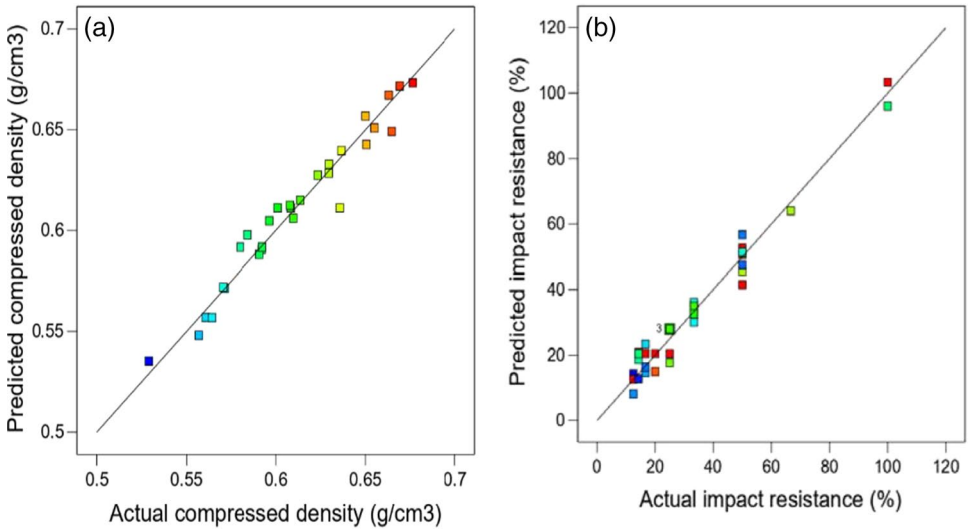

Fig. 9 Predicted vs. actual plots (**a**) compressed density (**b**) impact resistance

Table 6 Analysis of variance result for compressed density

Source	Sum of squares	df	Mean square	*F*-value	*p*-value	
Model	0.0393	15	0.0026	19.37	< 0.0001*	Significant
A-binder ratio	0.0106	1	0.0106	78.17	< 0.0001*	
B-particle size	0.0114	1	0.0114	83.96	< 0.0001*	
C-dwell time	0.0010	1	0.0010	7.34	0.0178*	
D-binder type	0.0012	2	0.0006	4.41	0.0345*	
AB	0.0005	1	0.0005	3.55	0.0821	
AC	0.0043	1	0.0043	31.68	< 0.0001*	
AD	0.0009	2	0.0005	3.49	0.0611	
BC	0.0002	1	0.0002	1.34	0.2672	
BD	0.0034	2	0.0017	12.50	0.0009*	
CD	0.0020	2	0.0010	7.41	0.0071*	
A^2	0.0028	1	0.0028	21.06	0.0005*	
Residual	0.0018	13	0.0001			
Lack of fit	0.0010	10	0.0001	0.4125	0.8737	Not significant
Pure error	0.0007	3	0.0002			
Cor total	0.0411	28				

*Significant at $p < 0.05$

Compressed density

$$\rho_{cp} = 0.528774 + 0.004836\text{A} - 0.039522\text{B} + 0.208071\text{C} - 0.003994\text{AB} - 0.010841\text{AC} - 0.027280\text{BC} + 0.000945A^2 \quad (17)$$

$$\rho_{cc} = 0.423572 + 0.005129\text{A} + 0.056579\text{B} + 0.153286\text{C} - 0.003994\text{AB} - 0.010841\text{AC} - 0.027280\text{BC} + 0.000945A^2 \quad (18)$$

$$\rho_{cl} = 0.583699 + 0.000402\text{A} - 0.025751\text{B} + 0.157397\text{C} - 0.003994\text{AB} - 0.010841\text{AC} - 0.027280\text{BC} + 0.000945A^2 \quad (19)$$

Impact resistance

$$I_P = -62.12624 - 15.57609\text{A} + 168.05516\text{B} + 20.35031\text{C} - 1.34217\text{AB} + 1.19074\text{AC} - 31.45639\text{BC} + 0.940964A^2 - 38.17509B^2 + 13.10722C^2 \quad (20)$$

Table 7 Analysis of variance result for impact resistance

Source	Sum of squares	df	Mean square	*F*-value	*p*-value	
Model	16,414.07	17	965.53	28.88	< 0.0001*	Significant
A-binder ratio	6434.87	1	6434.87	192.45	< 0.0001*	
B-particle size	96.13	1	96.13	2.88	0.1072	
C-dwell time	462.14	1	462.14	13.82	0.0016*	
D-binder type	1640.75	2	820.37	24.54	< 0.0001*	
AB	116.17	1	116.17	3.47	0.0787	
AC	43.23	1	43.23	1.29	0.2704	
AD	3677.20	2	1838.60	54.99	< 0.0001*	
BC	635.47	1	635.47	19.01	0.0004*	
BD	133.76	2	66.88	2.00	0.1643	
CD	459.56	2	229.78	6.87	0.0061*	
A^2	3979.56	1	3979.56	119.02	< 0.0001*	
B^2	599.57	1	599.57	17.93	0.0005*	
C^2	78.66	1	78.66	2.35	0.1425	
Residual	601.85	18	33.44			
Lack of fit	566.66	14	40.48	4.60	0.0756	Not significant
Pure error	35.19	4	8.80			
Cor total	17,015.92	35				

*Significant at $p < 0.05$

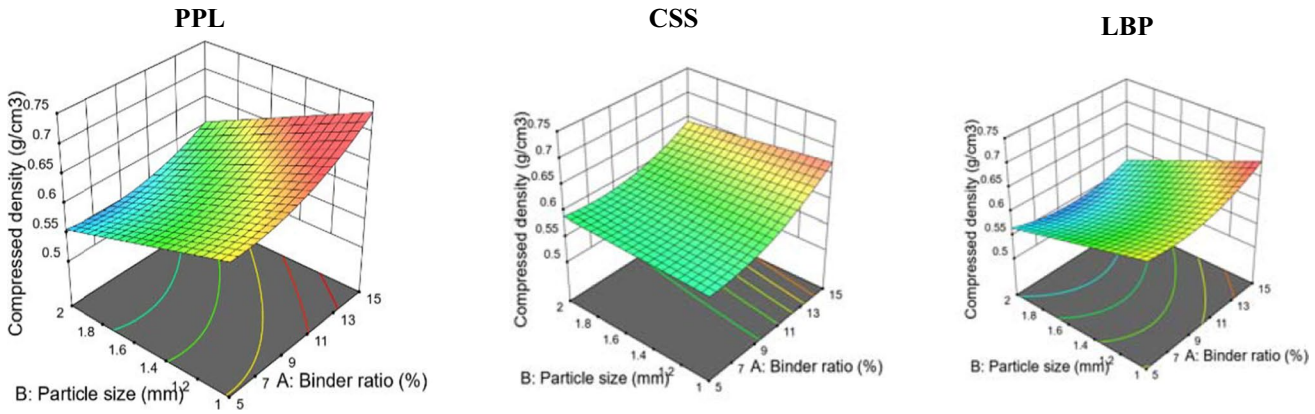

Fig. 10 The effect of interaction between particle size and binder ratio on compressed density

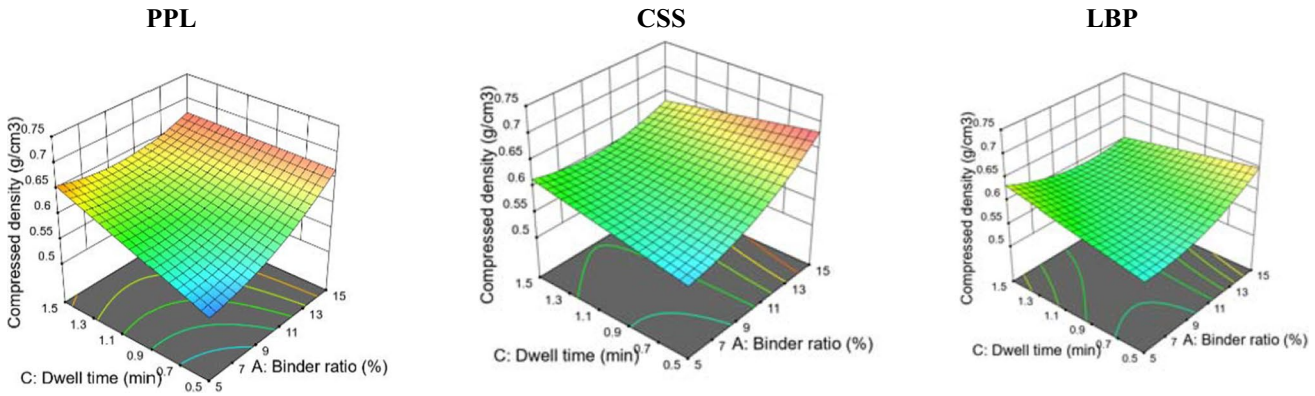

Fig. 11 The effect of interaction between dwell time and binder ratio on compressed density

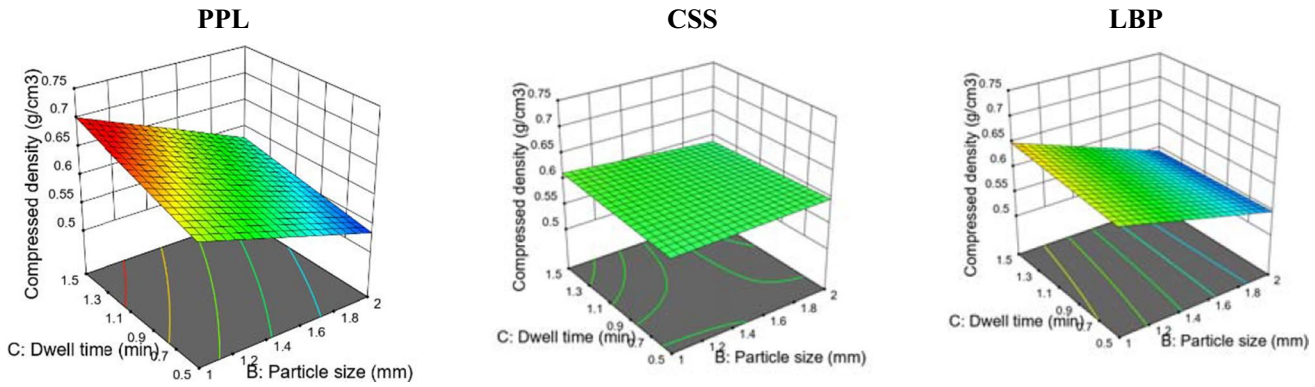

Fig. 12 The effect of interaction between dwell time and particle size on compressed density

$$I_c = -63.45074 - 9.14156A + 158.80811B - 7.80191C - 1.34217AB + 1.19074AC - 31.45639BC + 0.940964A^2 - 38.17509B^2 + 13.10722C^2 \quad (21)$$

$$I_l = -34.83216 - 15.44200A + 170.12438B - 3.87267C - 1.34217AB + 1.19074AC - 31.45639BC + 0.940964A^2 - 38.17509B^2 + 13.10722C^2 \quad (22)$$

3.4 Response surface analysis

3.4.1 Compressed density

Figure 10, 11, and 12 shows the 3D model graphs of the various interactions between the independent variables and compressed density. The color region in the plots indicates the change in performance from the lowest (blue) to the highest (red). In Fig. 10, the effect of interaction between particle size and binder ratio is shown when dwell time is held constant for 1 min. As depicted, compressed density increased steadily as particle size decreased from 2 to 1 mm and as binder content increased from 5 to 15% in briquettes produced with binder PPL and LBP. However, in the case of CSS-bonded briquettes, only a slight increment was observed between the binder ratio of 5% and 10% and a major increment was noted between binder content of 10% and 15%. This is because as the rice husks particle size decreases, the surface area increases, which enhances the interparticle bond during homogenization and compression. [42] also affirmed that the density of briquettes increases as particle size decreases and equally noted that binder content influences the briquette's density. A similar observation was reported by Ndindeng et al. [67] for briquettes made from carbonized rice husks. Although the maximum compressed density was noted at PPL briquettes, the difference between CSS and LBP briquettes in terms of the interaction between particle size and binder ratio was not significant.

A non-linear interaction effect was observed between dwell time and binder ratio on compressed density (Fig. 11). In this case, the highest compressed density was achieved when the dwell time and binder ratio were at their maximum in PPL briquettes, which was because the rice husk particles interacted effectively with PPL binder during densification. This could be an influence of gelatinization with LBH extract which improved the binder's gelly form. However, for CSS and LBP briquettes, the highest density was recorded at the point where dwell time and binder content were 0.5 min and 15%, respectively. This shows that the effect of dwell time on the briquette's density is more evident in PPL briquettes and generally minimal compared to the effect of binder ratio. Overall, compressed density was observed to increase in all the briquette types as the binder ratio increases. A similar trend was observed by Sanjika and Chipula [68] for briquettes of water hyacinth using a paper pulp binder. This is more typical in low-pressured briquetting where higher percentages of binder are required for adequate consolidation [28]. However, it is important to note that the effect of dwell time on briquettes quality depends on the type of biomass, binder, and the method of compression. In the case of the interaction between dwell time and particle size (Fig. 12), compressed density increases as dwell time increases and as particle size decreases. Similarly, the highest compressed density was noted at PPL briquettes implying a better interacting influence among the factors. Ajimotokan et al. [69] also observed that compressed density increases as particle size decreases. This indicates that the dwell time influences the compressed density positively and better when reacting with small particle sizes than when reacting with different binder content.

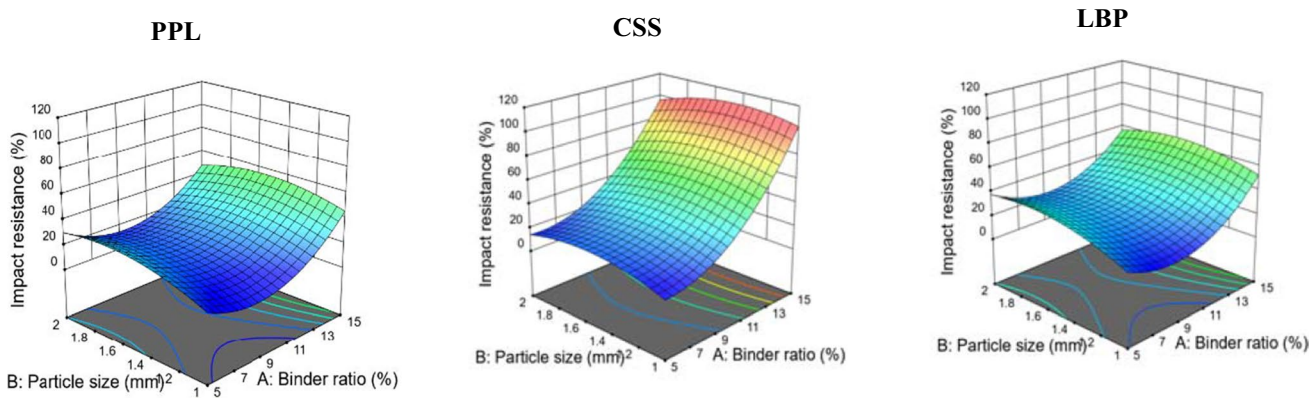

Fig. 13 The effect of interaction between particle size and binder ratio on impact resistance

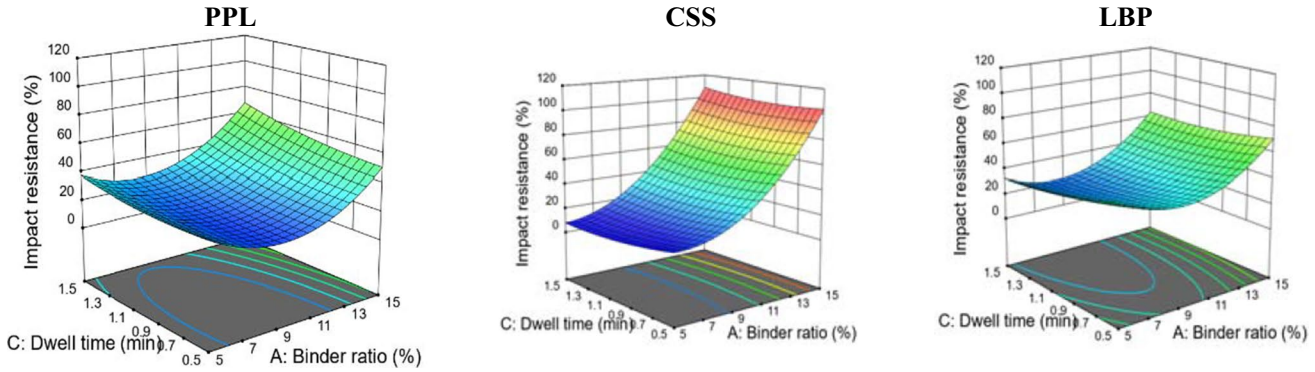

Fig. 14 The effect of interaction between dwell time and binder ratio on impact resistance

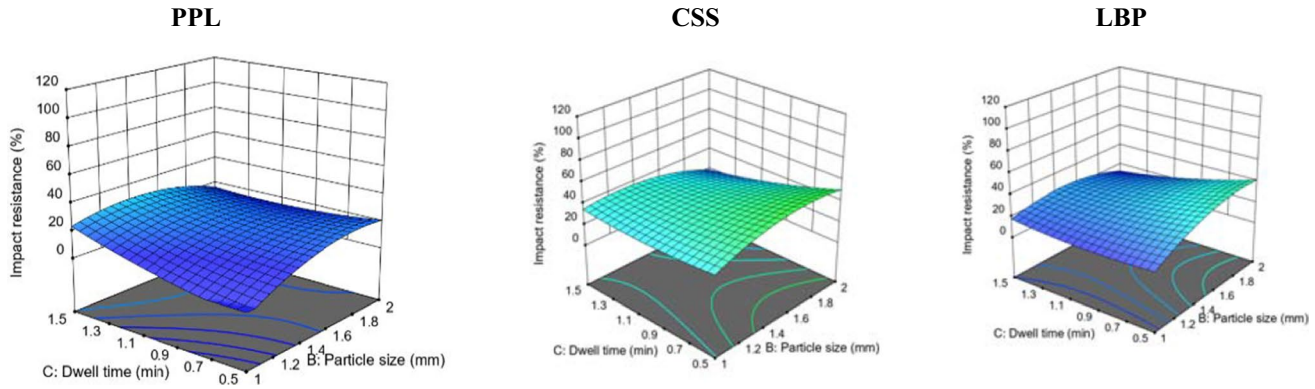

Fig. 15 The effect of interaction between dwell time and particle size on impact resistance

3.4.2 Impact resistance

The 3D model graphs of impact resistance are presented in Figs. 13, 14, and 15. In Fig. 13, the impact resistance was observed to increase sharply from 12.5% to a maximum level of 100% as the binder content increases and particle size decreases in CSS briquettes. TT et al. [41] also observed that impact resistance increases as particle size decreases. This implies that briquettes produced with small particle sizes have better strength and durability than those produced with large particle sizes. However, in PPL and LBP briquettes, the impact resistance decreased to a certain level within the particle size region of 1.4 to 2 mm and binder ratio of 5 to 11.5% before it increased to the peak maximum between

40 and 60% at 15% binder content region. CSS briquettes presented the highest impact resistance because cassava starch binder is more viscous and effective than PPL and LBP binders, based on which both the surface and core layer particles of the briquettes remain consolidated even after drying. Similarly, cassava starch contains amylose and amylopectin which enhances the briquette's resistance to heat and shear strength [29]. In Fig. 14, impact resistance as a function of dwell time and binder ratio is presented. In the figure, a slight decrease was observed at the initial phase before increasing rapidly to the maximum point where the binder content is 15%. This implies that, although the trend was not consistent, the highest impact resistance was noted at the point where the binder ratio is maximum in all the briquettes. Similarly, CSS briquettes had the highest impact resistance. With this, it becomes more evident that briquette's density and durability are two distinct quality parameters. Although dwell time influences impact resistance, especially in PPL and LBP briquettes, the influence of the ratio of binder is more evident in CSS briquettes. However, in Fig. 15, impact resistance was low between 12.5 and 40% depicting a minimal influence from the interaction between dwell time and particle size. In this vein, it shows that the strength of the briquettes is more evident when the binder interacts with another parameter than when it interacts with dwell time and particle size, inferring that binders are more essential in low-pressured briquette production. Overall, in this form of briquetting, the quality largely depends on the quality of the binder [17]. The highest impact resistance was observed when dwell time was lowest and particle size was between 1.3 and 2 mm in CSS and LBP briquettes. In the case of PPL briquettes, the highest impact resistance was recorded in the region of maximum dwell time (1.5-min) and particle size of 1.5 mm.

3.5 Optimization and validation

The optimization criteria employed in this paper were targeted at maximizing the response variables while maintaining the process parameters at the design range. The optimum process parameters are a 15% binder ratio, 1.1 mm particle size, 0.5-min dwell time, and cassava starch binder. Figure 16 shows the optimization plots of compressed density and impact resistance. An optimal compressed density of 0.689 g/cm^3 and impact resistance of 109.636% were predicted by the model. The obtained values represent the ideal process conditions that will reduce capital, maintenance, and operational costs [27], and give the most efficient output. This is important as there are multiple solutions obtained from the model. An overall desirability of 0.976 was obtained (Fig. 17). With a desirability approaching 1, it shows that the predicted values are very close to the ideal value.

To ascertain the veracity of the optimized parameters and responses, a validation experiment was conducted considering the optimal conditions obtained from the model. The average of the first three (3) solutions was considered for the validation (Table 7).

Table 8 shows the values obtained from the confirmatory experiment and those predicted by the model. With low percentage errors (< 10%), the difference between the confirmatory experiment and the predicted responses was minimal. Thus, confirming the validity of the optimization model. Further analysis using a *t*-test was employed to measure the deviation between the means (Table 9). With a *p*-value of

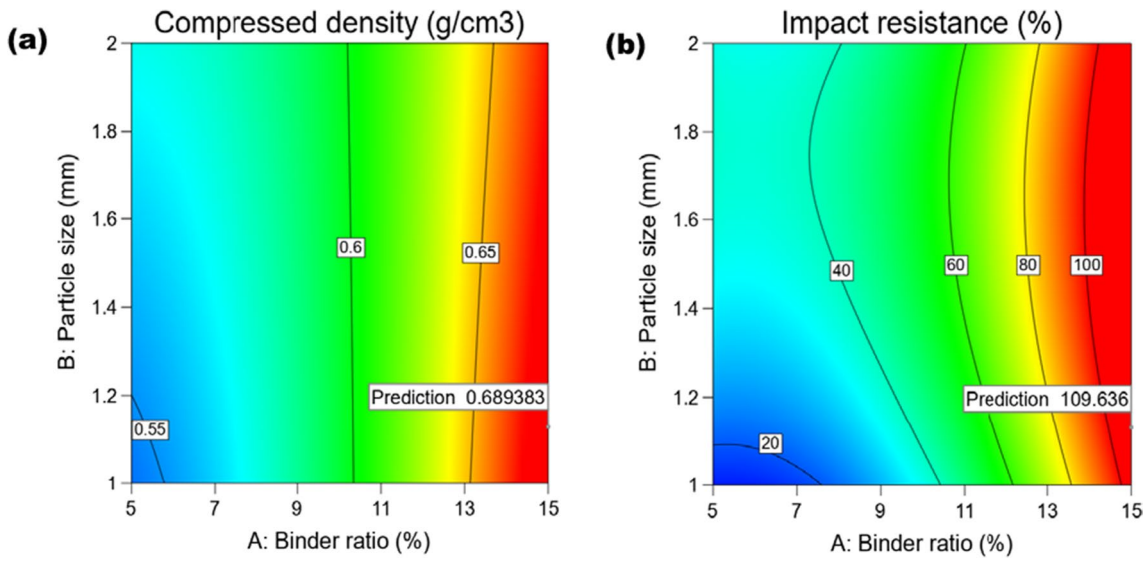

Fig. 16 Contour plots showing the optimized points: **a** compressed density, **b** impact resistance

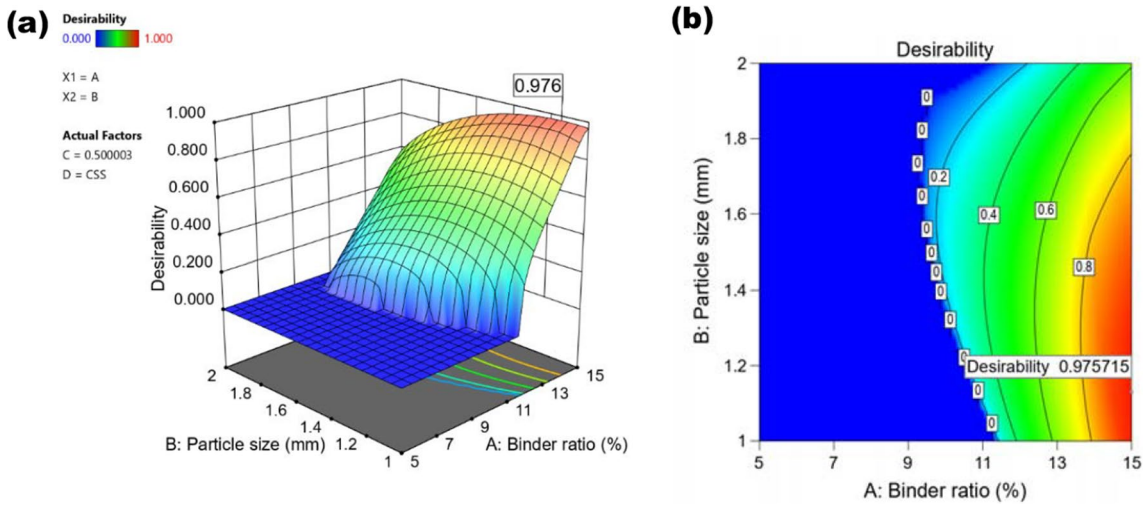

Fig. 17 Overall desirability graph: **a** 3D response surface plot. **b** contour plot

Table 8 Experimented and predicted values

Variable	Experimental value	Predicted value	Desirability	Error (%)
Comp. den. (g/cm^3)	0.582	0.689	0.976	
	0.699	0.689	0.976	
	0.699	0.689	0.976	
Average	***0.660***	***0.689***	***0.976***	***4.21***
Impact resistance (%)	100	109.636	0.976	
	100	109.641	0.976	
	100	109.411	0.976	
Average	***100***	***109.563***	***0.976***	***8.73***

0.498 (> 5%), it depicts that there is no significant difference between the experimented and predicted means.

4 Conclusion

Briquettes were developed from rice husk under low pressure (4.5 MPa) using novel biomass binders in this paper. While this was aimed at determining the optimal process conditions and quality response using RSM, it also assessed the potential of using locust bean pulp and sweet potato peel as binders in briquette production. This is essential as previous studies focus largely on inorganic and starch-based binders. The paper finds that to produce briquettes with rice husks at low pressure, 15% binder, 1.1-mm-particle size of rice husks, and 0.5-min residence time are optimum. With these optimal conditions, maximum predicted responses of 0.689 g/cm^3 compressed density and 109.6% impact resistance are achievable. The above predictions were validated experimentally and the differences between the experimental and predicted values were statistically insignificant at a 95% confidence interval. Similarly, the paper discovered that locust bean pulp and sweet potato peel can be used as binders in briquette production. However, more properties such as the starch, protein and sugar content of the binding materials needs to be explored further to comprehend the cohesivity.

In addition, the paper reveals that rice husk can be processed into briquettes without necessarily carbonizing or subjecting it to high pressure. This is critical for households relying heavily on fuelwood and spending a huge amount of time and resources in sourcing or purchasing fuelwood and charcoal as it shows that a low-cost production method is feasible. Based on this, with the large quantity of rice husk generated in Nigeria, rice husk briquettes can be sustainably produced at low pressure to reduce overreliance on fuelwood and charcoal and augment the energy shortfall in the country. This would not only save costs and provide a waste management strategy but would equally mitigate climate change. Although the paper is primarily focused on improving household energy use, the optimal conditions can be scaled up and applied at an industrial scale to achieve improved quality and output capacity. In this case,

Table 9 Summary of *t*-test analysis

	Obs	Mean1	Mean2	Dif	St err	*t* value	*p*-value
EV—PV	2	50.33	55.126	−4.796	4.767	−1	0.498

a multi-criteria optimization could be employed. Industries relying on coal and wood such as the cement and rice processing industries, could switch to the use of high-density briquettes. Here, machines within the pressure range of 50 to 100 MPa could be employed with a low proportion of binder. The higher the pressure, the lesser the binding requirement.

Future research should explore the possibility of processing two-stage rice husk into briquettes at low to medium pressure without milling the husk. In this case, the energy expended in milling will be saved and the overall production cost reduced. However, based on the pressure range, the ratio of binder may increase. Thus, evaluating distinctive design criteria and parameters is pertinent. Co-densifying rice husks and charcoal dust is another aspect that could be explored to reduce the effect of silica and ash in rice husks without necessarily carbonizing the husks, thereby enhancing the quality and thermal performance of the resulting briquettes. While carbonization could improve the thermal properties, it will surely affect the overall production life cycle. In this case, a comprehensive environmental life cycle assessment of rice husk briquette using different approaches is required to assess the impact of each process to determine the approach with the best quality and less environmental impact. Because the briquette machine used in this study is a constant pressure machine, the pressure level could not be varied. Thus, considering the pertinence of application pressure in briquette production, future studies could explore a broader pressure range through optimization to determine the optimum pressure for producing uncarbonized rice husk briquettes. This paper has evaluated selected biomass materials for briquette production based on the international wood pellet standard (ENplus). In addition, it revealed new binders for briquette production and the optimum process and response level in employing the binders in producing rice husk briquettes under low pressure. These findings could serve as a guide for future research and developments relating to household and industrial energy use, deforestation control, climate change mitigation, waste management, and recycling. In addition, it would assist policymakers and authorities advocating for net zero emission or carbon neutrality.

Acknowledgements The Authors are grateful to the German Federal Ministry of Education and Research (BMBF) for funding the study through the West African Science Service Centre on Climate Change and Adapted Land Use (WASCAL), under the Graduate Research Programme on Climate Change & Land Use (CCLU), College of Engineering, Kwame Nkrumah University of Science and Technology, Kumasi, Ghana. The Authors are also grateful to Ahmadu Bello University Zaria, Nigeria for granting the lead Author a study fellowship and a working space to carry out the experimental aspect of this study.

Author contribution All authors contributed to the study conception and design. Suleiman Usman Yunusa: conceptualization, methodology, investigation, writing—original draft; Ebenezer Mensah, Kwasi Preko, Satyanarayana Narra, Aminu Saleh: supervision, visualization, writing— review & editing; Ibrahim Babangida Dalha, Mohammed Abdulsalam: Formal analysis. All authors have read and agreed to the published version of the manuscript.

Funding This study was funded by the West African Science Service Centre on Climate Change and Adapted Land use (WASCAL) under the auspices of the German Federal Ministry of Education and Research (BMBF).

Data availability The data that support the findings of this study are openly available on request.

Declarations

Ethical approval Not applicable.

Competing interest The authors declare no competing interests.

References

1. United Nations General Assembly Economic and Social Council UN-ECOSOC (2024) Progress towards the sustainable development goals: report of the secretary-general. A/79/79-E2024/54. https://doi.org/10.1017/S0020818300010845
2. Yunusa SU, Mensah E, Preko K, Narra S, Saleh A, Sanfo S (2024) Assessing the nexus between household dynamics and cooking energy choice: evidence from Kaduna state, northwestern Nigeria. Energy Nexus 15:100310. https://doi.org/10.1016/j.nexus.2024.100310
3. Food and Agricultural Organization FAO (2022) The state of the world's forest: forest pathways for green recovery and building inclusive, resilient and sustainable economies. https://doi.org/10.4060/cb9360en. Accessed 1 Mar 2023
4. Liu Z, Zhang F, Liu H, Ba F, Yan S, Hu J (2018) Pyrolysis/gasification of pine sawdust biomass briquettes under carbon dioxide atmosphere: study on carbon dioxide reduction (utilization) and biochar briquettes physicochemical properties. Bioresour Technol 249:983–991. https://doi.org/10.1016/j.biortech.2017.11.012
5. Nikhom R, Suppalakpanya K, Nikhom S, Siriphan T (2024) Combustion properties improvement and economic evaluation of charcoal briquettes from mixed agricultural waste biomass. Biomass Convers Bior. https://doi.org/10.1007/s13399-024-05379-7
6. Jyothsna G, Bahurudeen A, Sahu PK (2024) Sustainable utilisation of rice husk for cleaner energy: a circular economy between agricultural, energy and construction sectors. Mater Today Sustain 25:100667. https://doi.org/10.1016/j.mtsust.2024.100667
7. Baetge S, Kaltschmitt M (2018) Rice straw and rice husks as energy sources—comparison of direct combustion and biogas production. Biomass Convers Biorefinery 8:719–737. https://doi.org/10.1007/s13399-018-0321-y
8. FAO (2021) Nigeria agriculture at a glance. FAO Niger 3–4. https://www.fao.org/nigeria/fao-in-nigeria/nigeria-at-a-glance/en/. Accessed 24 Jan 2022
9. Siddika A, Al MMA, Alyousef R, Mohammadhosseini H (2021) State-of-the-art-review on rice husk ash: A supplementary cementitious material in concrete. J King Saud Univ - Eng Sci 33:294–307. https://doi.org/10.1016/j.jksues.2020.10.006
10. Japhet JA, Luka BS, Maren IB, Datau SG (2020) The potential of wood and agricultural waste for pellet fuel development in Nigeria – a technical review. Int J Eng Appl Sci Technol 04:598–607. https://doi.org/10.33564/ijeast.2020.v04i11.105

11. Wang Z, Huang W, Wang H, Gao J, Zhang R, Xu G, Wang Z (2024) Research on the improvement of carbon neutrality by utilizing agricultural waste: based on a life cycle assessment of biomass briquette fuel heating system. J Clean Prod 434:140365. https://doi.org/10.1016/j.jclepro.2023.140365
12. Sugebo B (2022) A review on enhanced biofuel production from coffee by-products using different enhancement techniques. Mater Renew Sustain Energy 11:91–103. https://doi.org/10.1007/s40243-022-00209-0
13. Simões LMS, Setter C, Sousa NG, Cardoso CR, de Oliveira TJP (2024) Biomass to biofuel densification of coconut fibers: kinetic triplet and thermodynamic evaluation. Biomass Convers Biorefinery 14:631–648. https://doi.org/10.1007/s13399-022-02393-5
14. Njezic Z, Cvetkovic B, Kormanjos S, Banjac V, Zivkovic J (2014) Briquetting and pelleting the biomass: protection from fire and explosions. Zast Mater 55:86–90. https://doi.org/10.5937/zasmat1401086n
15. Yunusa SU, Mensah E, Preko K, Narra S, Saleh A, Sanfo S, Isiaka M, Dalha IB, Abdulsalam M (2023) Biomass cookstoves : a review of technical aspects and recent advances. Energy Nexus 11:100225. https://doi.org/10.1016/j.nexus.2023.100225
16. Brunerová A, Brožek M, Van Dung D, Phung LD, Hasanudin U, Iryani DA, Chaloupková V, Roubík H (2024) Manual wooden low-pressure briquetting press: an alternative technology of waste biomass utilisation in developing countries of Southeast Asia. J Clean Prod 436:140624. https://doi.org/10.1016/j.jclepro.2024.140624
17. Zhang G, Sun Y, Xu Y (2018) Review of briquette binders and briquetting mechanism. Renew Sustain Energy Rev 82:477–487. https://doi.org/10.1016/j.rser.2017.09.072
18. Kpalo SY, Zainuddin MF, Manaf LA, Roslan AM (2020) A review of technical and economic aspects of biomass briquetting. Sustainability 12:4609. https://doi.org/10.3390/su12114609
19. Obi OF, Pecenka R, Clifford MJ (2022) A review of biomass briquette binders and quality parameters. Energies 15:2426. https://doi.org/10.3390/en15072426
20. Muazu RI, Stegemann JA (2017) Biosolids and microalgae as alternative binders for biomass fuel briquetting. Fuel 194:339–347. https://doi.org/10.1016/j.fuel.2017.01.019
21. Magnago RF, Costa SC, Assunção Ezirio MJ de, Godoy Saciloto V de, Cremona Parma GO, Gasparotto ES, Gonçalves AC, Tutida AY, Barcelos RL (2020) Briquettes of citrus peel and rice husk. J Clean Prod 276:123820. https://doi.org/10.1016/j.jclepro.2020.123820
22. Yank A, Ngadi M, Kok R (2016) Physical properties of rice husk and bran briquettes under low pressure densification for rural applications. Biomass Bioenerg 84:22–30. https://doi.org/10.1016/j.biombioe.2015.09.015
23. Sunnu AK, Adu-Poku KA, Ayetor GK (2021) Production and characterization of charred briquettes from various agricultural waste. Combust Sci Technol. https://doi.org/10.1080/00102202.2021.1977803
24. Oladosu KO, Babalola SA, Kareem MW, Ajimotokan HA, Kolawole MY, Issa WA, Olawore AS, Ponle EA (2023) Optimization of fuel briquette made from bi-composite biomass for domestic heating applications. Sci African 21:e01824. https://doi.org/10.1016/j.sciaf.2023.e01824
25. Nganko JM, Koffi EPM, Gbaha P, Toure AO, Kane M, Ndiaye B, Faye M, Nkounga WM, Tiogue Tekounegning C, Bile EEJ, Yao KB (2024) Modeling and optimization of compaction pressure, binder percentage and retention time in the production process of carbonized sawdust-based biofuel briquettes using response surface methodology (RSM). Heliyon 10:e25376. https://doi.org/10.1016/j.heliyon.2024.e25376
26. Guo Z, Wu J, Zhang Y, Cao K, Feng Y, Liu J, Li J (2020) Briquetting optimization method for the lignite powder using response surface analysis. Fuel 267:117260. https://doi.org/10.1016/j.fuel.2020.117260
27. Marreiro HMP, Peruchi RS, Lopes RMBP, Rotella Junior P (2024) Briquetting process optimization of poultry litter and urban wood waste. Renew Energy 222:119955. https://doi.org/10.1016/j.renene.2024.119955
28. Yunusa SU, Mensah E, Preko K, Narra S, Saleh A, Sanfo S (2023) A comprehensive review on the technical aspects of biomass briquetting. Biomass Convers Biorefinery. https://doi.org/10.1007/s13399-023-04387-3
29. Lubwama M, Yiga VA (2018) Characteristics of briquettes developed from rice and coffee husks for domestic cooking applications in Uganda. Renew Energy 118:43–55. https://doi.org/10.1016/j.renene.2017.11.003
30. Suryaningsih S, Nurhilal O, Yuliah Y, Salsabila E (2018) Fabrication and characterization of rice husk charcoal bio briquettes. AIP Conf Proc 1927:030044. https://doi.org/10.1063/1.5021237
31. Dhankhar P (2014) Rice Milling. IOSR J Eng 4:34–42. https://doi.org/10.9790/3021-04543442
32. Awoyale AA, Lokhat D, Eloka-Eboka AC (2021) Experimental characterization of selected Nigerian lignocellulosic biomasses in bioethanol production. Int J Ambient Energy 42:1343–1351. https://doi.org/10.1080/01430750.2019.1594375
33. Auta SM, Solomon BU, Tsado TY (2015) Effect of locust bean pod extract (lbpe) as a replacement for water on the compressive strength of concrete. In: 1st international conference on green engineering sustainable development IC-GESD, vol 1. pp 119–123
34. Akande FB, Adejumo OA, Adamade CA, Bodunde J (2010) Processing of locust bean fruits: challenges and prospects. African J Agric Res 5:2268–2271
35. Miao Z, Zhang P, Li M, Wan Y, Meng X (2019) Briquette preparation with biomass binder. Energy Sources, Part A Recover Util Environ Eff 45:9834–9844. https://doi.org/10.1080/15567036.2019.1682722
36. ASTM D5865–10a (2010) Standard Test method for gross calorific value of coal and coke. In: Annu B ASTM Stand, pp 1–14. https://doi.org/10.1520/D5865-10A.2
37. ASTM D3173–87 (1996) Standard test method for moisture in the analysis sample of coal and coke. In: Annu B ASTM Stand, West Conshohocken, USA, pp 315–316
38. ASTMD3175 (2011) Standard test method for volatile matter in the analysis sample of coal and coke. ASTM Int 6. https://doi.org/10.1520/D3175-07.2
39. ASTM D3174–02 (2002) ASTM: Standard test method for ash in the analysis sample of coal and coke from coal. In: Annu B ASTM Stand West Conshohocken, PA, US. www.astm.org
40. Mitchual SJ, Frimpong-mensah K, Darkwa NA (2014) Evaluation of fuel properties of six tropical hardwood timber species for briquettes. J Sustain Bioenergy Syst 4:1–9. https://doi.org/10.4236/jsbs.2014.41001
41. Ak TT, Mech N, Ramesh ST, Gandhimathi R (2022) Evaluation of composite briquettes from dry leaves in energy applications for agrarian communities in India. J Clean Prod 350:131312. https://doi.org/10.1016/j.jclepro.2022.131312
42. Kipngetich P, Kiplimo R, Tanui JK, Chisale PC (2022) Optimization of combustion parameters of carbonized rice husk briquettes in a fixed bed using RSM technique. Renew Energy 198:61–74. https://doi.org/10.1016/j.renene.2022.07.130
43. ASTM D2395–17 (2017) Standard test methods for density and specific gravity (relative density) of wood and wood-based materials. In: ASTM Int., West Conshohocken, PA, USA. https://doi.org/10.1520/D2395-17

44. Gendek A, Aniszewska M, Malaťák J, Velebil J (2018) Evaluation of selected physical and mechanical properties of briquettes produced from cones of three coniferous tree species. Biomass Bioenerg 117:173–179. https://doi.org/10.1016/j.biombioe.2018.07.025
45. Richards SR (1990) Physical testing of fuel briquettes. Fuel Process Technol 25:89–100
46. ASTM D440 - 86 (2002) Standard test method of drop shatter test for coal. In: ASTM Int West Conshohocken, USA
47. Mitchual SJ, Frimpong-mensah K, Darkwa NA (2014) Relationship between physico-mechanical properties, compacting pressure and mixing proportion of briquettes produced from Maize Cobs and Sawdust. J Sustain Bioenergy Syst 4:50–60. https://doi.org/10.4236/jsbs.2014.41005
48. Barik D, Murugan S (2016) Experimental investigation on the behavior of a DI diesel engine fueled with raw biogas–diesel dual fuel at different injection timing. J Energy Inst 89:373–388. https://doi.org/10.1016/j.joei.2015.03.002
49. Dalha IB, Koca K, Said MA, Rafindadi AD (2024) Biogas intake pressure and port air swirl optimization to enhance the diesel RCCI engine characteristics for low environmental emissions. Process Saf Environ Prot 184:703–719. https://doi.org/10.1016/j.psep.2024.02.038
50. Asamoah B, Nikiema J, Gebrezgabher S, Odonkor E, Njenga M (2016) A review on production, marketing and use of fuel briquettes, Colombo, Sri Lanka. https://doi.org/10.5337/2017.200
51. International Organization for Standardization ISO 17225–1 (2020) Solid biofuels — fuel specifications and classes — Part 1: general requirements. https://www.iso.org/standard/76088.html. Accessed 19 Mar 2024
52. Yunusa SU, Narra S, Mensah E, Preko K, Aminu S (2024) Physical and thermochemical properties of selected wood species in Nigeria: a fuel suitability and pelleting potential assessment. Fuels 5:261–277. https://doi.org/10.3390/fuels5030015
53. Lubwama M, Yiga VA, Ssempijja I, Lubwama HN (2023) Thermal and mechanical characteristics of local firewood species and resulting charcoal produced by slow pyrolysis. Biomass Convers Bior 13:6689–6704. https://doi.org/10.1007/s13399-021-01840-z
54. Nikiema J, Asamoah B, Egblewogbe MNYH, Akomea-agyin J, Cofie OO, Felix A, Gebreyesus G, Zipporah K, Njenga M (2022) Impact of material composition and food waste decomposition on characteristics of fuel briquettes. Resour Conserv Recycl Adv 15:200095. https://doi.org/10.1016/j.rcradv.2022.200095
55. Nagarajan J, Prakash L (2021) Preparation and characterization of biomass briquettes using sugarcane bagasse, corncob and rice husk. Mater Today Proc 47:4194–4198. https://doi.org/10.1016/j.matpr.2021.04.457
56. Wang C, Zhang S, Wu S, Sun M, Lyu J (2020) Multi-purpose production with valorization of wood vinegar and briquette fuels from wood sawdust by hydrothermal process. Fuel 282:118775. https://doi.org/10.1016/j.fuel.2020.118775
57. Wang Q, Han K, Qi J, Zhang J, Li H, Lu C (2018) Investigation of potassium transformation characteristics and the influence of additives during biochar briquette combustion. Fuel 222:407–415. https://doi.org/10.1016/j.fuel.2018.02.156
58. Espuelas S, Marcelino S, Echeverría AM, del Castillo JM, Seco A (2020) Low energy spent coffee grounds briquetting with organic binders for biomass fuel manufacturing. Fuel 278:118310. https://doi.org/10.1016/j.fuel.2020.118310
59. Abedi A, Cheng H, Dalai AK (2018) Effects of natural additives on the properties of sawdust fuel pellets. Energy Fuels 32:1863–1873. https://doi.org/10.1021/acs.energyfuels.7b03663
60. Kumar A, Mohanta K, Kumar D, Parkash O (2012) Properties and industrial applications of rice husk: a review. Int J Emerg Technol Adv Eng 2
61. Kariuki SW, Wachira J, Kawira M, Murithi G (2020) Crop residues used as lignocellulose materials for particleboards formulation. Heliyon 6:e05025. https://doi.org/10.1016/j.heliyon.2020.e05025
62. Yunusa SU, Wakili BS (2023) Development of lignocellulosic-plastic composite from rice husk and polyethylene. Clean Circ Bioeconomy 6:100054. https://doi.org/10.1016/j.clcb.2023.100054
63. Mitchual SJ, Frimpong-mensah K, Darkwa NA, Akowuah JO (2013) Briquettes from maize cobs and Ceiba pentandra at room temperature and low compacting pressure without a binder. Int J Energy Environ 4:38
64. Falemara BC, Joshua VI, Aina OO, Nuhu RD (2018) Performance evaluation of the physical and combustion properties of briquettes produced from agro-wastes and wood residues. Recycling 3. https://doi.org/10.3390/recycling3030037
65. Fadele OK, Amusan TO, Afolabi AO, Ogunlade CA (2021) Characterisation of briquettes from forest wastes optimisation approach. Res Agric Eng 67:138–147. https://doi.org/10.17221/6/2021-RAE
66. Sakthivadivel D, Iniyan S (2020) Characterization, density and size effects of fuels in an advanced micro-gasifier stove. Biofuels 11:857–869. https://doi.org/10.1080/17597269.2018.1426163
67. Ndindeng SA, Mbassi JEG, Mbacham WF, Manful J, Graham-Acquaah S, Moreira J, Dossou J, Futakuchi K (2015) Quality optimization in briquettes made from rice milling by-products. Energy Sustain Dev 29:24–31. https://doi.org/10.1016/j.esd.2015.09.003
68. Sanjika T, Chipula G (2021) Technical feasibility of producing binder-free water hyacinth briquettes for domestic energy use. African J Sci Technol Innov Dev. https://doi.org/10.1080/20421338.2021.1988417
69. Ajimotokan HA, Ibitoye SE, Odusote JK, Adesoye OA, Omoniyi PO (2019) Physico-mechanical properties of composite briquettes from corncob and rice husk. J Bioresour Bioprod 4:159–165. https://doi.org/10.12162/jbb.v4i3.004